

Casimir energy of N δ -plates with constant conductivity

Venkat Abhignan

Qdit Labs Pvt. Ltd., Bengaluru - 560092, India

The Casimir energy for N δ -function plates depends on multiple scattering parameter Δ . This N body interaction was distributed into two body interactions with nearest neighbour scattering and next-to-nearest neighbour scattering based on partitions of $N - 1$ and its permutations. Implementing this methodology, we investigate Casimir energy for multiple plates with constant conductivity relatable to Graphene. We also study Casimir interaction between a perfect magnetic conductor and multiple constant conductivity δ plates, which results in Boyer repulsion. In the asymptotic limit for ideal boundary conditions, the results become simple where multiple scattering parameter Δ consists only of nearest neighbour scattering term.

I. INTRODUCTION

Casimir showed that there is a force between two parallel, perfectly conducting plates when there are quantum electrodynamic fluctuations in a vacuum [1]. Consecutively, it was shown for two dielectric slabs with finite conductivity [2]. It is acknowledged that the non-additivity of this interaction makes it difficult to calculate Casimir energies and related Lifshitz forces for multiple dielectric bodies [3, 4], even if exact results have been obtained for ideal boundary conditions.

Casimir forces dominate in nano- or micro-structures, causing stiction [5, 6]. Casimir energies can be expressed using the multiple scattering formalism in terms of the reflection coefficients of the structure [7–10]. A single layer of Graphene is called Graphene, where carbon atoms align to create a two-dimensional hexagonal lattice [11]. Graphene, with its miniaturized structure and unique optical properties [12] can be utilized to modulate Casimir forces by modifying reflection coefficients [13–16].

Tomaš initially pursued the Casimir force for parallel multilayered structures [17, 18]. Casimir energy for N layers of Graphene with optical Fresnel coefficients had been handled recently using this approach [19]. The initial study for N layers of Graphene considered a scalar model and was solved using the mode-summation approach with zeta function regularisation [20]. Other than these formalisms, the Piston approach [21], the Modal approach [22], the path-integral approach [23] and the plasma sheets model [24] have been applied to study Casimir energy for multilayers. However, no closed-form Casimir calculation for N bodies exists. Adding more layers results in complex expressions and difficulty when dealing with multiple dielectric cavities.

Casimir energy of N magnetodielectric δ -function plates was predicted recently using multiple scattering formalism and stress-tensor method [25]. δ -function plates [26] and related plasma sheet model [27, 28] have been developed exclusively to study 2D materials like Graphene. In this work, we calculate the Casimir energy of Graphene multilayers using δ -function plates with constant and isotropic optical conductivity [29]. The optical response of Graphene, which is essential for Casimir calculations, is determined by its electronic structure and Dirac-like carriers [15, 30]. The optical conductivity is independent of all material parameters in the limit $\hbar\omega \leq 3eV$ [31]. The optical absorption is a meagre 2.3% at room temperature, depending only on the fine structure constant $\alpha = 1/137$ [32]. Also, if spatial dispersion can be ignored, the conductivity is isotropic [33].

In Sec.II, we describe the method to obtain generalized expression for Casimir energy between N δ -plates and obtain closed-form expression of Casimir energy for $N = 6$ plates with different properties. In Sec. III, we calculate and analyze the Casimir energy of $N = 2, \dots, 6$ plates with constant conductivity relevant to Graphene. In Sec. IV, we investigate the repulsive Casimir forces resulting in an interaction between infinitely permeable material and δ plates with constant conductivity.

II. CASIMIR ENERGY OF N MAGNETODIELECTRIC δ -PLATES

The multiple scattering parameter $\Delta_{12\dots N}$ can describe the Casimir energy $\Delta E_{(12\dots N)}$ of N plates such as [25]

$$\frac{\Delta E_{(12\dots N)}}{A} = \frac{1}{2} \int_{-\infty}^{\infty} \frac{d\zeta}{2\pi} \int \frac{d^2 k_{\perp}}{(2\pi)^2} \left[\ln \left[\Delta_{12\dots N}^H \right] + \ln \left[\Delta_{12\dots N}^E \right] \right], \quad (1)$$

integrated over all wavenumbers and frequencies (with superscript E denoting TE mode and H for TM mode).

The parameter $\Delta_{12\dots N}$ can be distributed into the nearest neighbour scattering parameter Δ_{ij} , and the next-to-nearest neighbour, next-to-next-to-nearest neighbour, \dots scattering parameters Δ_{ik} based on partitions of $N - 1$

and its permutations (Further, described with an example for $N = 6$). The characteristics of scattering parameters indicate the various ways the propagation may contribute to the energy. Δ_{ij} and Δ_{ik} can be produced by visualizing a diagrammatic loop distribution with an exponential dependence on the distance between the plates l_{ij} , and in terms of the optical properties of the plates with reflection and transmission coefficients r_i and t_i such as,

$$r_i^H = -\frac{\lambda_{gi}^\perp \zeta^2}{\lambda_{gi}^\perp \zeta^2 + 2\kappa} + \frac{\lambda_{ei}^\perp \kappa}{\lambda_{ei}^\perp \kappa + 2}, \quad t_i^H = 1 - \frac{\lambda_{gi}^\perp \zeta^2}{\lambda_{gi}^\perp \zeta^2 + 2\kappa} - \frac{\lambda_{ei}^\perp \kappa}{\lambda_{ei}^\perp \kappa + 2} \quad (2)$$

with $\kappa = \sqrt{k_\perp^2 + \zeta^2}$. Coefficients r^E, t^E corresponding to TE mode can be obtained by replacing superscripts $H \rightarrow E$ and by swapping $\lambda_{ei}^\perp \leftrightarrow \lambda_{gi}^\perp$. The matrix

$$\boldsymbol{\lambda}_{e,g}(\zeta) = \begin{bmatrix} \lambda_{e,g}^\perp(\zeta) & 0 & 0 \\ 0 & \lambda_{e,g}^\perp(\zeta) & 0 \\ 0 & 0 & 0 \end{bmatrix} \quad (3)$$

describes the electric properties $\boldsymbol{\lambda}_e$ and magnetic properties $\boldsymbol{\lambda}_g$ corresponding to $\boldsymbol{\varepsilon}$ and $\boldsymbol{\mu}$ of the material, respectively (with planar symmetry, implying isotropic and homogeneous on the plate) in Heaviside–Lorentz units. Based on these coefficients, the nearest neighbour scattering parameters Δ_{ij} are

$$\Delta_{ij} = 1 - r_i e^{-\kappa l_{ij}} r_j e^{-\kappa l_{ij}}, \quad (4)$$

for $j = i + 1$ ($i \in [1, N - 1]$ where i and j are adjacent plates) and next-to-next-to-nearest neighbour, \dots scattering parameters Δ_{ik} are

$$\Delta_{ik} = -r_i e^{-\kappa l_{i,i+1}} t_{i+1} e^{-\kappa l_{i+1,i+2}} t_{i+2} \dots e^{-\kappa l_{k-1,k}} r_k e^{-\kappa l_{k-1,k}} \dots t_{i+1} e^{-\kappa l_{i,i+1}}, \quad (5)$$

for $k \geq i + 2$ ($i \in [1, N - 2]$ where i and k are not adjacent plates). Δ_{ij} only depends on the reflection coefficients of neighbouring plates i, j with exponential dependence of length between the plates. Δ_{ik} depends on the reflection coefficients of bordering plates i, k and transmission coefficients of nearby adjacent plates $i + 1, \dots, k - 1$ between the bordering plates as the propagation happens with exponential length dependence.

For example, the Casimir energy of $N = 6$ plates configuration, which is usually hard to handle, depends only on multiple scattering parameter Δ_{123456} . This term can be separated based on partitions of $N - 1 = 5$ as

$$\begin{aligned} \Delta_{123456} = & \Delta_{12}\Delta_{23}\Delta_{34}\Delta_{45}\Delta_{56} + \Delta_{12}\Delta_{24}\Delta_{45}\Delta_{56} + \Delta_{13}\Delta_{34}\Delta_{45}\Delta_{56} + \Delta_{12}\Delta_{23}\Delta_{35}\Delta_{56} + \Delta_{12}\Delta_{23}\Delta_{34}\Delta_{46} + \Delta_{13}\Delta_{35}\Delta_{56} \\ & + \Delta_{13}\Delta_{34}\Delta_{46} + \Delta_{12}\Delta_{24}\Delta_{46} + \Delta_{12}\Delta_{23}\Delta_{36} + \Delta_{12}\Delta_{25}\Delta_{56} + \Delta_{14}\Delta_{45}\Delta_{56} + \Delta_{14}\Delta_{46} + \Delta_{13}\Delta_{36} + \Delta_{15}\Delta_{56} + \Delta_{12}\Delta_{26} + \Delta_{16} \end{aligned} \quad (6)$$

and Fig. 1 illustrates the diagrammatic loop distribution of this multiple scattering parameter. Understanding the propagation of multiple scattering formalism is easier with the help of this pattern. The partitions of 5 are (5), (4,1), (3,2), (3,1,1), (2,2,1), (2,1,1,1) and (1,1,1,1,1). In Eq.(6), it can be intuitively understood that term corresponding to partition (5) is Δ_{16} and partition (1,1,1,1,1) is $\Delta_{12}\Delta_{23}\Delta_{34}\Delta_{45}\Delta_{56}$. Similarly, terms corresponding to partition (4,1), (1,4) are $\Delta_{15}\Delta_{56}, \Delta_{12}\Delta_{26}$ and partition (3,2), (2,3) are $\Delta_{14}\Delta_{46}, \Delta_{13}\Delta_{36}$, respectively. Terms corresponding to partition (1,1,3), (1,3,1), (3,1,1) are $\Delta_{12}\Delta_{23}\Delta_{36}, \Delta_{12}\Delta_{25}\Delta_{56}, \Delta_{14}\Delta_{45}\Delta_{56}$, respectively. Terms corresponding to partition (2,2,1), (2,1,2), (1,2,2) are $\Delta_{13}\Delta_{35}\Delta_{56}, \Delta_{13}\Delta_{34}\Delta_{46}, \Delta_{12}\Delta_{24}\Delta_{46}$, respectively. And terms corresponding to partition (1,2,1,1), (2,1,1,1), (1,1,2,1), (1,1,1,2) are $\Delta_{12}\Delta_{24}\Delta_{45}\Delta_{56}, \Delta_{13}\Delta_{34}\Delta_{45}\Delta_{56}, \Delta_{12}\Delta_{23}\Delta_{35}\Delta_{56}, \Delta_{12}\Delta_{23}\Delta_{34}\Delta_{46}$, respectively.

Further, using Eq.s (4) and (5) in this multiple scattering parameter Eq. (6) for $N = 6$ plates in terms of optical properties in Eq. (2) gives

$$\begin{aligned} \Delta_{123456} = & (1 - r_1 r_2 e^{-2\kappa a}) (1 - r_2 r_3 e^{-2\kappa a}) (1 - r_3 r_4 e^{-2\kappa a}) (1 - r_4 r_5 e^{-2\kappa a}) (1 - r_5 r_6 e^{-2\kappa a}) \\ & - (1 - r_1 r_2 e^{-2\kappa a}) r_2 t_3^2 r_4 e^{-4\kappa a} (1 - r_4 r_5 e^{-2\kappa a}) (1 - r_5 r_6 e^{-2\kappa a}) - r_1 t_2^2 r_3 e^{-4\kappa a} (1 - r_3 r_4 e^{-2\kappa a}) (1 - r_4 r_5 e^{-2\kappa a}) (1 - r_5 r_6 e^{-2\kappa a}) \\ & - (1 - r_1 r_2 e^{-2\kappa a}) (1 - r_2 r_3 e^{-2\kappa a}) r_3 t_4^2 r_5 e^{-4\kappa a} (1 - r_5 r_6 e^{-2\kappa a}) - (1 - r_1 r_2 e^{-2\kappa a}) (1 - r_2 r_3 e^{-2\kappa a}) (1 - r_3 r_4 e^{-2\kappa a}) r_4 t_5^2 r_6 e^{-4\kappa a} \\ & + r_1 t_2^2 r_3^2 t_4^2 r_5 e^{-8\kappa a} (1 - r_5 r_6 e^{-2\kappa a}) + r_1 t_2^2 r_3 (1 - r_3 r_4 e^{-2\kappa a}) r_4 t_5^2 r_6 e^{-8\kappa a} + (1 - r_1 r_2 e^{-2\kappa a}) r_2 t_3^2 r_4^2 t_5^2 r_6 e^{-8\kappa a} \\ & - (1 - r_1 r_2 e^{-2\kappa a}) (1 - r_2 r_3 e^{-2\kappa a}) r_3 t_4^2 t_5^2 r_6 e^{-6\kappa a} - (1 - r_1 r_2 e^{-2\kappa a}) r_2 t_3^2 t_4^2 r_5 e^{-6\kappa a} (1 - r_5 r_6 e^{-2\kappa a}) \\ & - r_1 t_2^2 t_3^2 r_4 e^{-6\kappa a} (1 - r_4 r_5 e^{-2\kappa a}) (1 - r_5 r_6 e^{-2\kappa a}) + r_1 t_2^2 t_3^2 r_4^2 t_5^2 r_6 e^{-10\kappa a} + r_1 t_2^2 t_3^2 t_4^2 t_5^2 r_6 e^{-10\kappa a} - r_1 t_2^2 t_3^2 t_4^2 r_5 e^{-8\kappa a} (1 - r_5 r_6 e^{-2\kappa a}) \\ & - (1 - r_1 r_2 e^{-2\kappa a}) r_2 t_3^2 t_4^2 t_5^2 r_6 e^{-8\kappa a} - r_1 t_2^2 t_3^2 t_4^2 t_5^2 r_6 e^{-10\kappa a} \quad (7) \end{aligned}$$

with constant length $l_{ij} = a$ between the plates.

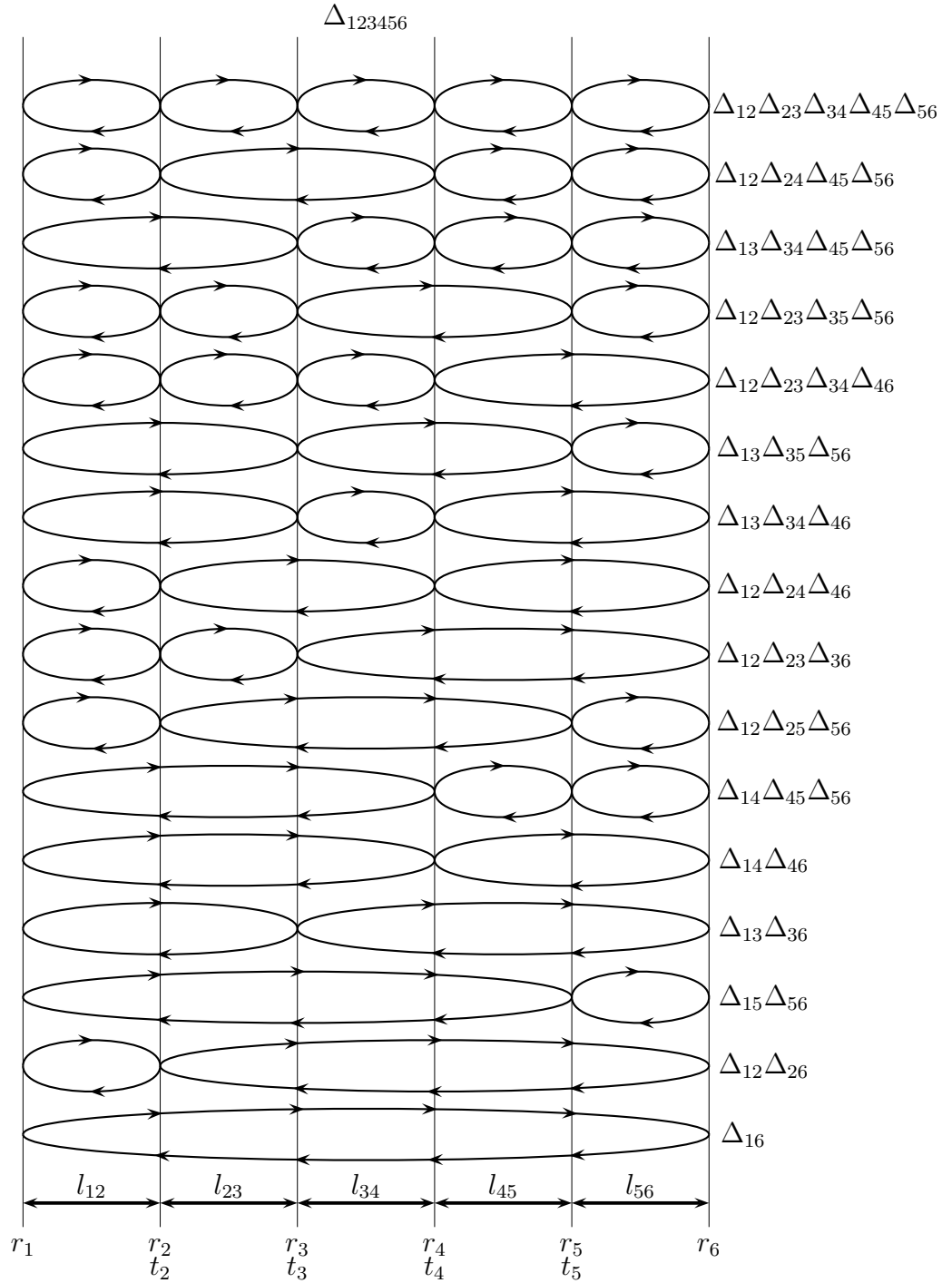


FIG. 1: Multiple scattering parameter Δ_{123456} is illustrated by partitions consisting of nearest neighbour scattering and next-to-nearest neighbour scattering. Each scattering term is defined in a tractable manner from the visualization of the loop based on the optical properties of the plates denoted by r_i and t_i , the reflection and transmission coefficients, respectively, along with the distance between the plates where i and j are adjacent is denoted by l_{ij} . For instance, term $\Delta_{36} = r_3 e^{-\kappa l_{34}} t_4 e^{-\kappa l_{45}} t_5 e^{-\kappa l_{56}} r_6 e^{-\kappa l_{56}} t_5 e^{-\kappa l_{45}} t_4 e^{-\kappa l_{34}}$ from Eq. (5) refers to loop between plates $i = 3$ and $k = 6$ with initial reflection r_3 , propagation with exponential dependence of length l_{34} , transmission t_4 , propagation of length l_{45} , transmission t_5 , propagation of length l_{56} , reflection with r_6 , again propagation of length l_{56} , transmission with t_5 , propagation of length l_{45} , transmission t_4 , propagation of length l_{34} and it continues.

III. CASIMIR ENERGY BETWEEN CONSTANT CONDUCTIVITY δ -PLATES

Based on massless Dirac model [15, 30] for constant isotropic conductivity σ and an dielectric medium with finite thickness d ,

$$(\epsilon^\perp(\zeta) - 1)d = \frac{\sigma}{\zeta} \text{ where at the thin plate limit [26] } \lim_{d \rightarrow 0} (\epsilon^\perp(\zeta) - 1)d = \lambda_e^\perp(\zeta) \quad (8)$$

which gives the optical property of δ -plate. With this, the reflection and transmission coefficients from Eq. (2) are

$$r_\sigma^H = \frac{\sigma\kappa}{\sigma\kappa + 2\zeta}, \quad r_\sigma^E = -\frac{\sigma\zeta}{\sigma\zeta + 2\kappa} \text{ and } t_\sigma^H = 1 - \frac{\sigma\kappa}{\sigma\kappa + 2\zeta}, \quad t_\sigma^E = 1 - \frac{\sigma\zeta}{\sigma\zeta + 2\kappa}, \quad (9)$$

with no magnetic property $\lambda_g^\perp = 0$. Using this the Casimir energy of $N = 2$ plates with constant conductivity from Eq. (1) is

$$\frac{\Delta E_{(12)}}{A} = \frac{1}{2} \int_{-\infty}^{\infty} \frac{d\zeta}{2\pi} \int \frac{d^2 k_\perp}{(2\pi)^2} \left[\ln \left[1 - \left(\frac{\sigma\kappa}{\sigma\kappa + 2\zeta} \right)^2 e^{-2\kappa a} \right] + \ln \left[1 - \left(-\frac{\sigma\zeta}{\sigma\zeta + 2\kappa} \right)^2 e^{-2\kappa a} \right] \right] \quad (10)$$

from considering $r_{1,2} = r_\sigma$, $r_{3,4,5,6} = 0$ in Eq. (7). Taking the asymptotic limit $\sigma \rightarrow \infty$ we obtain the Casimir energy between two perfectly conducting plates as $\Delta E_{(12)}^c/A = -\pi^2/720a^3$. Introducing spherical polar coordinates $k_\perp = \kappa \sin\theta$ and $\zeta = \kappa \cos\theta$ [34] in Eq. (10) we obtain

$$\frac{\Delta E_{(12)}}{\Delta E_{(12)}^c} = -\frac{45}{2\pi^4} \int_0^1 dt \int_0^\infty s^2 ds \left[\ln \left[1 - \left(\frac{\sigma}{\sigma + 2t} \right)^2 e^{-s} \right] + \ln \left[1 - \left(-\frac{\sigma}{\sigma + \frac{2}{t}} \right)^2 e^{-s} \right] \right] \quad (11)$$

scaled with $\Delta E_{(12)}^c$. Evaluation of s integral yields

$$\frac{\Delta E_{(12)}}{\Delta E_{(12)}^c} = \frac{45}{\pi^4} \int_0^1 dt \left[\text{Li}_4 \left(\frac{\sigma}{\sigma + 2t} \right)^2 + \text{Li}_4 \left(-\frac{\sigma}{\sigma + \frac{2}{t}} \right)^2 \right] \quad (12)$$

where $\text{Li}_4(z)$ is a polylogarithm function and numerical evaluation of Eq. (12) considering $\sigma = \pi a$ for Graphene gives $\Delta E_{(12)} = 0.00538 \Delta E_{(12)}^c$ as shown previously in Ref. [16].

Similarly, the Casimir energy of $N = 3$ plates from Eq. (1) is

$$\begin{aligned} \frac{\Delta E_{(123)}}{A} = & \frac{1}{2} \int_{-\infty}^{\infty} \frac{d\zeta}{2\pi} \int \frac{d^2 k_\perp}{(2\pi)^2} \left[\ln \left[1 - 2 \left(\frac{\sigma\kappa}{\sigma\kappa + 2\zeta} \right)^2 e^{-2\kappa a} + \right. \right. \\ & \left. \left. \left(\left(\frac{\sigma\kappa}{\sigma\kappa + 2\zeta} \right)^4 - \left(\frac{\sigma\kappa}{\sigma\kappa + 2\zeta} \right)^2 \left(1 - \frac{\sigma\kappa}{\sigma\kappa + 2\zeta} \right)^2 \right) e^{-4\kappa a} \right] \right. \\ & \left. + \ln \left[1 - 2 \left(-\frac{\sigma\zeta}{\sigma\zeta + 2\kappa} \right)^2 e^{-2\kappa a} + \left(\left(-\frac{\sigma\zeta}{\sigma\zeta + 2\kappa} \right)^4 - \left(-\frac{\sigma\zeta}{\sigma\zeta + 2\kappa} \right)^2 \left(1 - \frac{\sigma\zeta}{\sigma\zeta + 2\kappa} \right)^2 \right) \right] e^{-4\kappa a} \right] \quad (13) \end{aligned}$$

from considering $r_{1,2,3} = r_\sigma$, $t_2 = t_\sigma$, $r_{4,5,6} = 0$ in Eq. (7). Introducing the spherical polar coordinates and evaluation of s integral gives

$$\begin{aligned} \frac{\Delta E_{(123)}}{\Delta E_{(12)}^c} = & \frac{45}{\pi^4} \int_0^1 dt \left[\text{Li}_4 \left(\frac{2b_1}{\sqrt{a_1^2 - 4b_1} - a_1} \right) + \text{Li}_4 \left(-\frac{2b_1}{\sqrt{a_1^2 - 4b_1} - a_1} \right) \right] \\ & + \left[\text{Li}_4 \left(\frac{2b_2}{\sqrt{a_2^2 - 4b_2} - a_2} \right) + \text{Li}_4 \left(-\frac{2b_2}{\sqrt{a_2^2 - 4b_2} - a_2} \right) \right] \right], \quad (14) \end{aligned}$$

where

$$a_1 = -2 \left(\frac{\sigma}{\sigma + 2t} \right)^2, \quad b_1 = \left(\frac{\sigma}{\sigma + 2t} \right)^4 - \left(\frac{\sigma}{\sigma + 2t} \right)^2 \left(1 - \frac{\sigma}{\sigma + 2t} \right)^2, \quad a_2 = -2 \left(-\frac{\sigma}{\sigma + \frac{2}{t}} \right)^2, \\ b_2 = \left(-\frac{\sigma}{\sigma + \frac{2}{t}} \right)^4 - \left(-\frac{\sigma}{\sigma + \frac{2}{t}} \right)^2 \left(1 - \frac{\sigma}{\sigma + \frac{2}{t}} \right)^2. \quad (15)$$

Further, numerical evaluation using $\sigma = \pi\alpha$ yields Casimir energy for $N = 3$ Graphene plates as $\Delta E_{(123)} = 0.011\Delta E_{(12)}^c$. In a similar manner we evaluate Casimir energy of $N = 4, 5, 6$ Graphene plates as $\Delta E_{(1234)} = 0.017\Delta E_{(12)}^c$, $\Delta E_{(12345)} = 0.022\Delta E_{(12)}^c$, $\Delta E_{(123456)} = 0.028\Delta E_{(12)}^c$. In Fig. 2, the energy of $N = 2, 3, 4, 5, 6$ plates

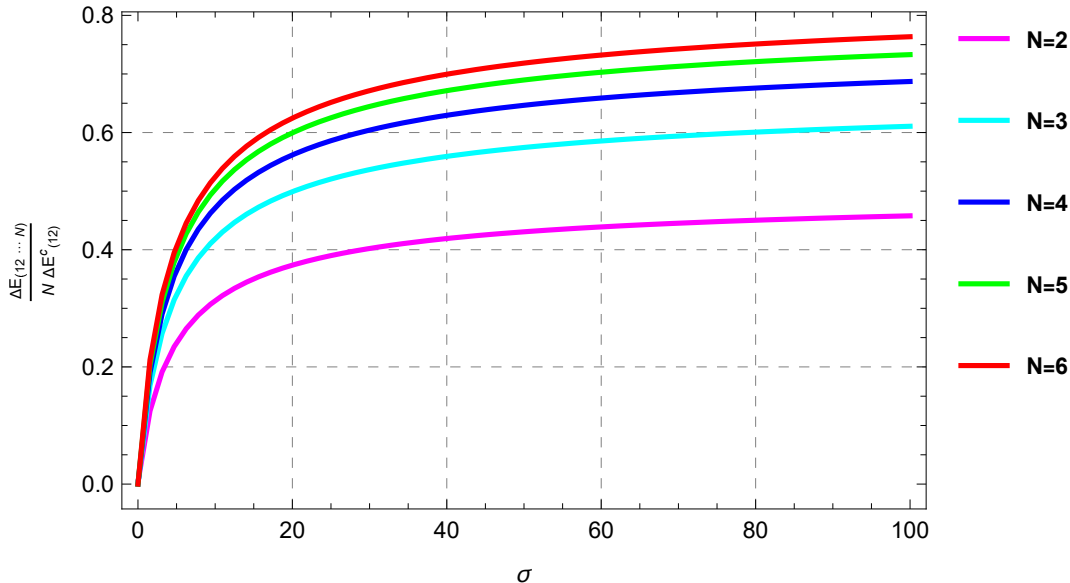


FIG. 2: Casimir energy of $N = 2, 3, 4, 5, 6$ plates scaled by $E_{(12)}^c$ and normalised per unit plate N for varying σ .

scaled by $E_{(12)}^c$ and normalised per unit plate N is displayed to understand how the energy behaves for different values of σ . The energy $\Delta E_{(12...N)}/N$ approaches the $E_{(12)}^c$ for two perfectly conducting plates as $N \gg 1$ which was previously seen in Ref. [20]. This is in the case of ideal boundary conditions like perfectly conducting plates (Dirichlet boundary conditions [35]) because the Casimir energy of N plates in Eq. (1) only involves the nearest neighbour scattering parameters Δ_{ij} in Eq. (4). The analysis is simple when the next-to-next-to-nearest neighbour, \dots scattering parameters Δ_{ik} in Eq. (5) do not contribute, and it can be evaluated in a straightforward manner that

$$E_{(12...N)}^c = (N - 1)E_{(12)}^c \quad (16)$$

(In the asymptotic limit $\sigma \rightarrow \infty$) as also shown in Ref. [25]. Consecutively $E_{(12...N)}^c/N \rightarrow E_{(12)}^c$ for $N \gg 1$.

IV. CASIMIR ENERGY BETWEEN INFINITELY PERMEABLE AND DIELECTRIC δ -PLATES

In direct contrast to Casimir's result of attractive force [1], Boyer discovered repulsive force from the interaction between a pure dielectric material and a pure magnetic conductor as $E_{(12)}^b = -7/8E_{(12)}^c$ [36]. This is evident from the optical coefficients of δ plate with an infinitely permeable material from Eq. (2) where $r_g^H = -1, r_g^E = 1$ and $t_g^{H,E} = 0$ for $\lambda_g^\perp \rightarrow \infty$, whereas optical coefficients of δ plate with an infinitely dielectric material are $r_e^H = 1, r_e^E = -1$ and $t_e^{H,E} = 0$ for $\lambda_e^\perp \rightarrow \infty$. Using this the Casimir energy of $N = 2$ plates from Eq. (1) with $r_1 = r_e, r_2 = r_g, r_{3,4,5,6} = 0$ in Eq. (7) leads to

$$\frac{\Delta E_{(12)}^b}{A} = \frac{1}{2} \int_{-\infty}^{\infty} \frac{d\zeta}{2\pi} \int \frac{d^2 k_\perp}{(2\pi)^2} \left[\ln \left[1 + e^{-2\kappa a} \right] + \ln \left[1 + e^{-2\kappa a} \right] \right]. \quad (17)$$

Evaluating this gives $\Delta E_{(12)}^b/A = 7/8(\pi^2/720a^3)$ leading to a repulsive force.

Interestingly, the Casimir energy for N δ plates with alternating pure electric and magnetic properties (Zaremba boundary conditions with alternating Dirichlet and Neumann boundary conditions in scalar case [37]) also leads to

$$\Delta E_{(12\dots N)}^b = (N-1)E_{(12)}^b \quad (18)$$

since transmission coefficients $t_g^{H,E} = 0$ and $t_e^{H,E} = 0$, where next-to-next-to-nearest neighbour, \dots scattering parameters Δ_{ik} in Eq. (5) do not contribute.

Also, while Casimir energy of $N = 2$ plates from Eq. (1) with $r_1 = r_e, r_2 = r_\sigma, r_{3,4,5,6} = 0$ in Eq. (7) leads to

$$\frac{\Delta E_{(12)}}{A} = \frac{1}{2} \int_{-\infty}^{\infty} \frac{d\zeta}{2\pi} \int \frac{d^2 k_\perp}{(2\pi)^2} \left[\ln \left[1 - \left(\frac{\sigma\kappa}{\sigma\kappa + 2\zeta} \right) e^{-2\kappa a} \right] + \ln \left[1 - \left(\frac{\sigma\zeta}{\sigma\zeta + 2\kappa} \right) e^{-2\kappa a} \right] \right], \quad (19)$$

and evaluating with $\sigma = \pi\alpha$ gives an attractive force of $\Delta E_{(12)} = 0.027\Delta E_{(12)}^c$ between a Graphene plate and perfect dielectric material. Whereas, Casimir energy from Eq. (1) with $r_1 = r_g, r_2 = r_\sigma, r_{3,4,5,6} = 0$ in Eq. (7) leads to

$$\frac{\Delta E_{(12)}}{A} = \frac{1}{2} \int_{-\infty}^{\infty} \frac{d\zeta}{2\pi} \int \frac{d^2 k_\perp}{(2\pi)^2} \left[\ln \left[1 + \left(\frac{\sigma\kappa}{\sigma\kappa + 2\zeta} \right) e^{-2\kappa a} \right] + \ln \left[1 + \left(\frac{\sigma\zeta}{\sigma\zeta + 2\kappa} \right) e^{-2\kappa a} \right] \right], \quad (20)$$

and evaluating it gives an repulsive force of $\Delta E_{(12)} = -0.026\Delta E_{(12)}^c$ between a Graphene plate and perfect magnetic permeable material. The energy leads to repulsive force whenever $r_1^{H,E} r_2^{H,E} < 0$.

Further, we study the effect of an infinitely permeable plate within a stack and outside a stack of finitely conducting plates in Casimir energy of $N = 3, 4, 5, 6$ from Eq. (1). Casimir energy of $N = 3$ plates with $r_1 = r_g, r_{2,3} = r_\sigma, r_{4,5,6} = 0$ and $r_2 = r_g, r_{1,3} = r_\sigma, r_{4,5,6} = 0$ in Eq. (7) for varying conductivity σ is displayed in Fig. 3. We observe that for small values of σ the perfectly permeable plate adjacent to two consecutive constant conductivity plates causes repulsion force and as σ increases the force turns attractive. Meanwhile, the force is always repulsive when the perfectly permeable plate is between constant conductivity plates, as it physically disconnects the two spaces.

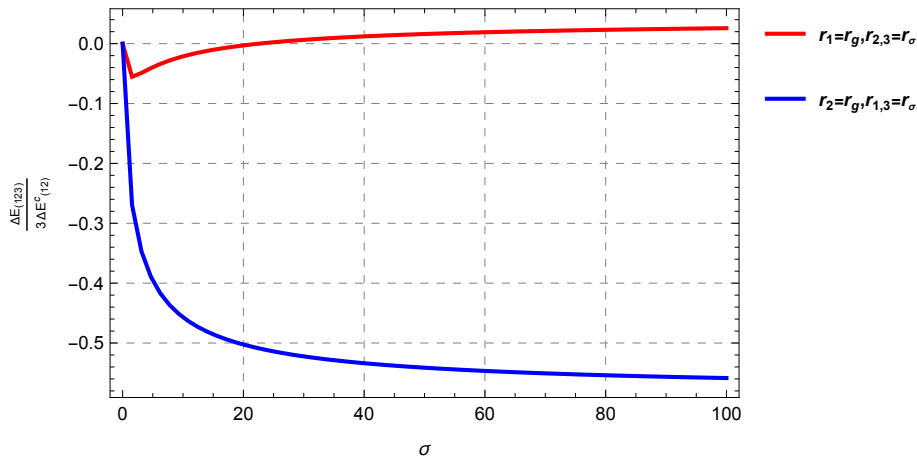


FIG. 3: Casimir energy of $N = 3$ plates with an infinitely permeable plate and for varying σ of other plates.

In the case of Casimir energy of $N = 4$ plates with a perfectly permeable plate adjacent to three constant conductivity plates ($r_1 = r_g, r_{2,3,4} = r_\sigma$) the force is always attractive. With a perfectly permeable plate in between three constant conductivity plates ($r_2 = r_g, r_{1,3,4} = r_\sigma$), the force is always repulsive as shown in Fig. 4. Similarly, the Casimir energy of $N = 5, 6$ plates are shown in Figs. 5, 6, where the perfectly permeable plate inside the stack causes a repulsive force only for smaller values of σ .

In the asymptotic limit for perfect metals ($\sigma \rightarrow \infty$), the values of Casimir energy can be easily evaluated from Eq.s (16) and (18). For instance, the Casimir energy for $N = 4$ when $\sigma \rightarrow \infty$ is $\Delta E_{(1234)} = (E_{(12)}^b + E_{(23)}^c + E_{(34)}^c)/4E_{(12)}^c = 0.28125$ for $r_1 = r_g, r_{2,3,4} = r_\sigma$ and $\Delta E_{(1234)} = (E_{(12)}^b + E_{(23)}^b + E_{(34)}^c)/4E_{(12)}^c = -0.1875$ for $r_2 = r_g, r_{1,3,4} = r_\sigma$ as can be seen in Fig. 4.

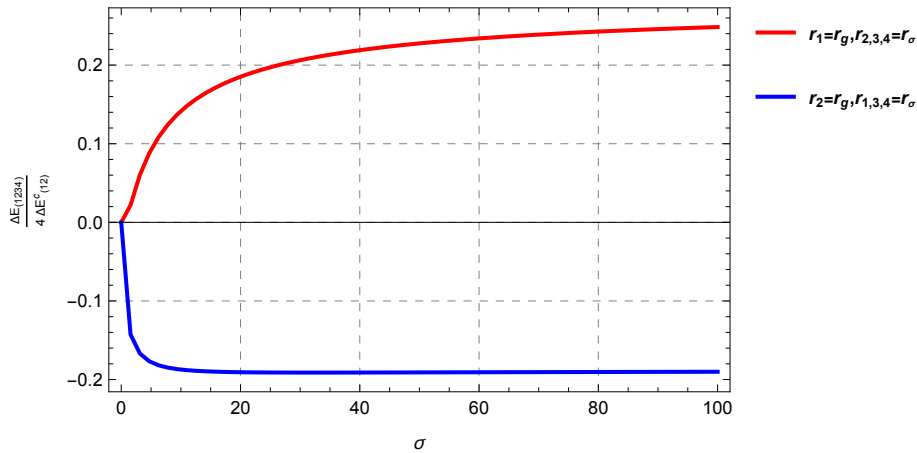


FIG. 4: Casimir energy of $N = 4$ plates with an infinitely permeable plate and for varying σ of other plates.

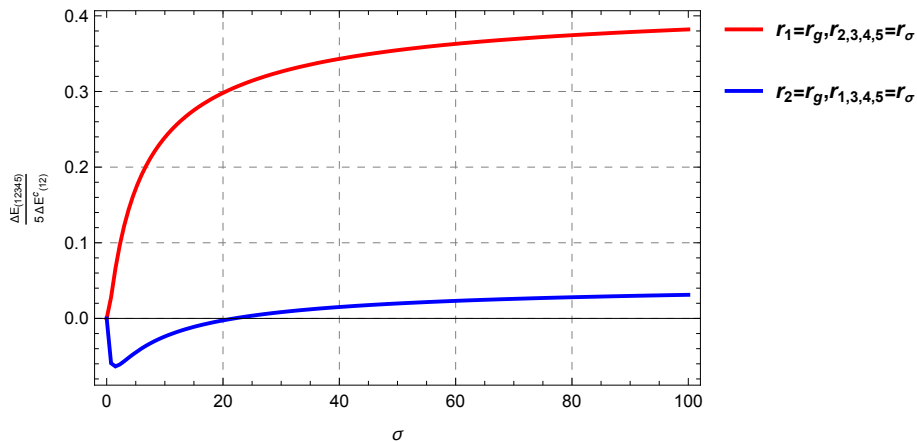


FIG. 5: Casimir energy of $N = 5$ plates with an infinitely permeable plate and for varying σ of other plates.

V. CONCLUSIONS

The Casimir energy for $N = 6$ δ -function plates was derived depending on multiple scattering parameter Δ ; the result for N plates may be easily generalized as described. Casimir energy of $N = 2, \dots, 6$ plates with Graphene-related constant conductivity was computed and numerically studied comparing with existing studies [16, 20]. Because of Graphene's transparency and finite optical conductivity, we found that the Casimir energy between graphene plates obeys the same distance dependence as the energy between two perfect electric conductors but with significantly smaller magnitudes. Further, experimentally relevant parameters like binding energies [19, 20] can perhaps be studied using the Drude-Lorentz model of conductivity for Graphene [38].

We also studied the interaction of infinitely permeable material and δ plates with constant conductivity, which results in repulsive Casimir forces. We observed the change in repulsive to attractive forces based on configuration and position of infinitely permeable δ plate in Casimir energy of $N = 3, \dots, 6$ plates. Boyer repulsion is interesting [39], but since naturally occurring materials do not exhibit strong magnetic responses, it has been regarded as non-physical and challenging [40, 41]. However, recent advancements in nanofabrication have produced metamaterials with magnetic responses [42], which may be relevant to the physical realization of Boyer's repulsion [43, 44]. Also, understanding the fundamental notion of electromagnetic force density turning negative (attractive force) to positive (repulsive force) is nontrivial [34, 45], which needs further investigation.

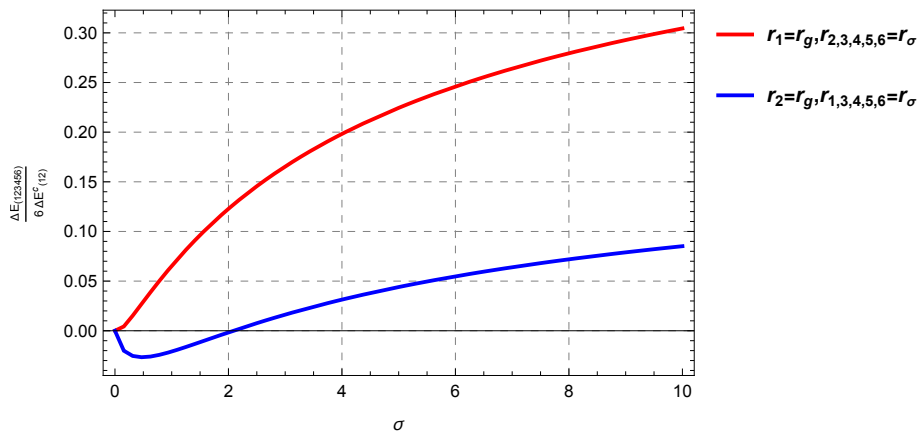


FIG. 6: Casimir energy of $N = 6$ plates with an infinitely permeable plate and for varying σ of other plates.

ACKNOWLEDGEMENTS

We are incredibly grateful to Dr. K. V. Shajesh and Dr. Prachi Parashar for introducing their work on δ -function plates and for further guidance.

-
- [1] H. B. G. Casimir, “On the Attraction Between Two Perfectly Conducting Plates,” *Kon. Ned. Akad. Wetensch. Proc.*, vol. 51, p. 793, 1948.
 - [2] E. M. Lifshitz, “The theory of molecular attractive forces between solids,” *Sov. Phys. JETP*, vol. 2, pp. 73–83, 1956.
 - [3] B. W. Ninham and V. A. Parsegian, “van der Waals Interactions in Multilayer Systems,” *The Journal of Chemical Physics*, vol. 53, pp. 3398–3402, 11 1970.
 - [4] B. W. Ninham and V. A. Parsegian, “van der Waals Forces across Triple-Layer Films,” *The Journal of Chemical Physics*, vol. 52, pp. 4578–4587, 05 1970.
 - [5] E. Buks and M. L. Roukes, “Stiction, adhesion energy, and the casimir effect in micromechanical systems,” *Phys. Rev. B*, vol. 63, p. 033402, Jan 2001.
 - [6] H. B. Chan, V. A. Aksyuk, R. N. Kleiman, D. J. Bishop, and F. Capasso, “Nonlinear micromechanical casimir oscillator,” *Phys. Rev. Lett.*, vol. 87, p. 211801, Oct 2001.
 - [7] R. Balian and B. Duplantier, “Electromagnetic waves near perfect conductors. I. Multiple scattering expansions. distribution of modes,” *Annals of Physics*, vol. 104, no. 2, pp. 300–335, 1977.
 - [8] R. Balian and B. Duplantier, “Electromagnetic waves near perfect conductors. II. Casimir effect,” *Annals of Physics*, vol. 112, no. 1, pp. 165–208, 1978.
 - [9] O. Kenneth and I. Klich, “Opposites attract: A theorem about the Casimir force,” *Phys. Rev. Lett.*, vol. 97, p. 160401, Oct 2006.
 - [10] T. Emig, N. Graham, R. L. Jaffe, and M. Kardar, “Casimir forces between arbitrary compact objects,” *Phys. Rev. Lett.*, vol. 99, p. 170403, Oct 2007.
 - [11] K. S. Novoselov, A. K. Geim, S. V. Morozov, D. Jiang, Y. Zhang, S. V. Dubonos, I. V. Grigorieva, and A. A. Firsov, “Electric field effect in atomically thin carbon films,” *Science*, vol. 306, no. 5696, pp. 666–669, 2004.
 - [12] A. H. Castro Neto, F. Guinea, N. M. R. Peres, K. S. Novoselov, and A. K. Geim, “The electronic properties of graphene,” *Rev. Mod. Phys.*, vol. 81, pp. 109–162, Jan 2009.
 - [13] J. F. Dobson, A. White, and A. Rubio, “Asymptotics of the dispersion interaction: Analytic benchmarks for van der Waals energy functionals,” *Phys. Rev. Lett.*, vol. 96, p. 073201, Feb 2006.
 - [14] G. Gómez-Santos, “Thermal van der Waals interaction between graphene layers,” *Phys. Rev. B*, vol. 80, p. 245424, Dec 2009.
 - [15] M. Bordag, I. V. Fialkovsky, D. M. Gitman, and D. V. Vassilevich, “Casimir interaction between a perfect conductor and graphene described by the dirac model,” *Phys. Rev. B*, vol. 80, p. 245406, Dec 2009.
 - [16] D. Drosdoff and L. M. Woods, “Casimir forces and graphene sheets,” *Phys. Rev. B*, vol. 82, p. 155459, Oct 2010.
 - [17] M. S. Tomaš, “Casimir force in absorbing multilayers,” *Phys. Rev. A*, vol. 66, p. 052103, 2002.
 - [18] M. S. Tomaš, “Casimir effect across a layered medium,” *International Journal of Modern Physics: Conference Series*, vol. 14, pp. 561–565, 2012.
 - [19] N. Emelianova, N. Khusnutdinov, and R. Kashapov, “Casimir effect for a stack of graphene sheets,” *Phys. Rev. B*, vol. 107, p. 235405, Jun 2023.

- [20] N. Khusnutdinov, R. Kashapov, and L. M. Woods, “Casimir effect for a stack of conductive planes,” *Phys. Rev. D*, vol. 92, p. 045002, Aug 2015.
- [21] L. P. Teo, “Casimir piston of real materials and its application to multilayer models,” *Phys. Rev. A*, vol. 81, p. 032502, Mar 2010.
- [22] P. S. Davids, F. Intravaia, F. S. S. Rosa, and D. A. R. Dalvit, “Modal approach to casimir forces in periodic structures,” *Phys. Rev. A*, vol. 82, p. 062111, Dec 2010.
- [23] E. Amooghorban, M. Wubs, N. A. Mortensen, and F. Kheirandish, “Casimir forces in multilayer magnetodielectrics with both gain and loss,” *Phys. Rev. A*, vol. 84, p. 013806, Jul 2011.
- [24] A. Allocca, S. Avino, S. Balestrieri, E. Calloni, S. Caprara, M. Carpinelli, L. D’Onofrio, D. D’Urso, R. De Rosa, L. Errico, G. Gagliardi, M. Grilli, V. Mangano, M. Marsella, L. Naticchioni, A. Pasqualetti, G. P. Pepe, M. Perciballi, L. Pesenti, P. Puppo, P. Rapagnani, F. Ricci, L. Rosa, C. Rovelli, D. Rozza, P. Ruggi, N. Saini, V. Sequino, V. Sipala, D. Stornaiuolo, F. Tafuri, A. Tagliacozzo, I. Tosta e Melo, and L. Trozzo, “Casimir energy for N superconducting cavities: a model for the YBCO (GdBCO) sample to be used in the Archimedes experiment,” *The European Physical Journal Plus*, vol. 137, no. 7, p. 826, 2022.
- [25] V. Abhignan, “Casimir energy of N magnetodielectric δ -function plates,” *Physica Scripta*, vol. 98, p. 105018, sep 2023.
- [26] P. Parashar, K. A. Milton, K. V. Shajesh, and M. Schaden, “Electromagnetic semitransparent δ -function plate: Casimir interaction energy between parallel infinitesimally thin plates,” *Phys. Rev. D*, vol. 86, p. 085021, Oct 2012.
- [27] G. Barton, “Casimir effects for a flat plasma sheet: I. energies,” *Journal of Physics A: Mathematical and General*, vol. 38, no. 13, pp. 2997–3019, 2005.
- [28] G. Barton, “Casimir effects for a flat plasma sheet: II. fields and stresses,” *Journal of Physics A: Mathematical and General*, vol. 38, p. 3021, mar 2005.
- [29] L. A. Falkovsky and A. A. Varlamov, “Space-time dispersion of graphene conductivity,” *The European Physical Journal B*, vol. 56, pp. 281–284, Apr 2007.
- [30] I. V. Fialkovsky and D. V. Vassilevich, “Graphene through the looking glass of QFT,” *Modern Physics Letters A*, vol. 31, no. 40, p. 1630047, 2016.
- [31] A. B. Kuzmenko, E. van Heumen, F. Carbone, and D. van der Marel, “Universal optical conductance of graphite,” *Phys. Rev. Lett.*, vol. 100, p. 117401, Mar 2008.
- [32] R. R. Nair, P. Blake, A. N. Grigorenko, K. S. Novoselov, T. J. Booth, T. Stauber, N. M. R. Peres, and A. K. Geim, “Fine structure constant defines visual transparency of graphene,” *Science*, vol. 320, no. 5881, pp. 1308–1308, 2008.
- [33] D. Drosdoff, A. D. Phan, L. M. Woods, I. V. Bondarev, and J. F. Dobson, “Effects of spatial dispersion on the casimir force between graphene sheets,” *The European Physical Journal B*, vol. 85, p. 365, Nov 2012.
- [34] I. Brevik, P. Parashar, and K. V. Shajesh, “Casimir force for magnetodielectric media,” *Phys. Rev. A*, vol. 98, p. 032509, Sep 2018.
- [35] K. V. Shajesh, I. Brevik, I. Cavero-Peláez, and P. Parashar, “Casimir energies of self-similar plate configurations,” *Phys. Rev. D*, vol. 94, p. 065003, Sep 2016.
- [36] T. H. Boyer, “Van der Waals forces and zero-point energy for dielectric and permeable materials,” *Phys. Rev. A*, vol. 9, pp. 2078–2084, May 1974.
- [37] M. Asorey and J. Muñoz-Castañeda, “Attractive and repulsive Casimir vacuum energy with general boundary conditions,” *Nuclear Physics B*, vol. 874, no. 3, pp. 852–876, 2013.
- [38] A. B. Djurišić and E. H. Li, “Optical properties of graphite,” *Journal of Applied Physics*, vol. 85, pp. 7404–7410, 05 1999.
- [39] O. Kenneth, I. Klich, A. Mann, and M. Revzen, “Repulsive Casimir forces,” *Phys. Rev. Lett.*, vol. 89, p. 033001, Jun 2002.
- [40] D. Iannuzzi and F. Capasso, “Comment on “repulsive Casimir forces”,,” *Phys. Rev. Lett.*, vol. 91, p. 029101, Jul 2003.
- [41] O. Kenneth, I. Klich, A. Mann, and M. Revzen, “Kenneth et al. reply:,” *Phys. Rev. Lett.*, vol. 91, p. 029102, Jul 2003.
- [42] V. M. Shalaev, “Optical negative-index metamaterials,” *Nature Photonics*, vol. 1, pp. 41–48, Jan 2007.
- [43] I. Pirozhenko and A. Lambrecht, “Repulsive Casimir forces and the role of surface modes,” *Phys. Rev. A*, vol. 80, p. 042510, Oct 2009.
- [44] V. Yannopoulos and N. V. Vitanov, “First-principles study of Casimir repulsion in metamaterials,” *Phys. Rev. Lett.*, vol. 103, p. 120401, Sep 2009.
- [45] J. S. Høyne and I. Brevik, “Repulsive Casimir force,” *Phys. Rev. A*, vol. 98, p. 022503, Aug 2018.